Activation by Serotonin and Noradrenaline of Vasopressin and Oxytocin Expression in the Mouse Paraventricular and Supraoptic Nuclei

Claire-Marie Vacher,[1] **Philippe Frétier,**[2] **Christophe Créminon,**[2] **André Calas,**[1] **and Hélène Hardin-Pouzet**[1]

[1]*Laboratory of Neurobiology of Intercellular Signals, Unité Mixte de Recherche 7101, Centre National de la Recherche Scientifique, Pierre and Marie Curie University, 75252 Paris Cedex 05, France, and* [2]*Commissionership to Atomic Energy, Service of Pharmacology and Immunology, 91191 Gif-sur-Yvette Cedex, France*

Noradrenaline and serotonin are known to control arginine-vasopressin (AVP) and oxytocin (OT) secretion in the systemic circulation. The aim of the current study was to investigate whether these monoamines are also able to influence AVP and OT expression in the paraventricular (PVN) and supraoptic nuclei (SON). To test this hypothesis, we used the Tg8 transgenic mice KO for the monoamine oxidase-A gene, which present high levels of noradrenaline and serotonin in the brain. AVP and OT expression were evaluated at peptide and mRNA levels by immunohistochemistry, enzyme immunoassay, and *in situ* hybridization. Compared with wild type, the amounts of AVP, OT, AVP mRNA, and OT mRNA were increased in the PVN and SON in Tg8 mice. To distinguish the respective contributions of noradrenaline and serotonin to these modifications, we treated Tg8 mice with a synthesis inhibitor of either catecholamines [α-methylparatyrosine (α-MPT)] or serotonin [parachlorophenylalanine (pCPA)]. Administration of α-MPT to Tg8 mice induced a decline in the amounts of AVP, OT, and their mRNA in the PVN and SON. The pCPA treatment in Tg8 mice was also associated with a decrease in OT expression in the PVN and SON and in AVP expression in the PVN, but not in the SON. These results suggest that noradrenaline may activate AVP and OT expression in the PVN and SON. Likewise, serotonin is proposed to stimulate AVP and OT expression in the PVN and only OT expression in the SON.

Key words: vasopressin; oxytocin; paraventricular nucleus; supraoptic nucleus; serotonin; noradrenaline; monoamine oxidase; transgenic mouse

The neurohypophyseal hormones arginine-vasopressin (AVP) and oxytocin (OT) are synthesized primarily in magnocellular perikarya of the paraventricular nucleus (PVN) and the supraoptic nucleus (SON) of the hypothalamus. AVP and OT are released from neurosecretory terminals to the systemic circulation at the level of the neurohypophysis. Plasmatic AVP regulates the extracellular fluid balance, and OT triggers both parturition and suckling-induced milk ejection (Cunningham and Sawchenko, 1991). A more restrained synthesis of these peptides exists in the parvocellular division of the PVN. In this region peptidergic neurons either deliver their secretion products to the portal blood system to stimulate adrenocorticotropic hormone (ACTH) secretion in response to stressful stimuli (Plotsky, 1987) or emit projections to the caudal medulla and the spinal cord to modulate multiple vegetative functions (Porter and Brody, 1986; Rogers and Herman, 1986; Siaud et al., 1991; Malpas and Coote, 1994; Hallbeck and Blomqvist, 1999; Giuliano and Rampin, 2000). The synthesis and the release of AVP and OT by the PVN and SON are stimulated by increased plasma osmolality (Sherman et al., 1983; Van Tol et al., 1987; Meister et al., 1990; Tracer and Loh, 1993; Amaya et al., 1999), hypovolemia (Stricker and Verbalis, 1986; Huang et al., 2001), suckling stimuli (Grosvenor and Mena,

1982; Zingg and Lefebvre, 1988), parturition (Douglas et al., 1998), or stress (Plotsky, 1987).

Morphological data have shown that the PVN and the SON represent the main hypothalamic targets for the noradrenergic system arising from A1/A2 and A6 cell groups of the brainstem (Sawchenko and Swanson, 1982; Cunningham and Sawchenko, 1988; Ginsberg et al., 1994). They also receive a moderate serotonergic innervation from the B7, B8, and B9 raphe nuclei (Sawchenko et al., 1983; Larsen et al., 1996). Electrophysiological and pharmacological studies indicate that these monoaminergic inputs play a critical excitatory role in the release of AVP and OT, in particular when an increased hormone level is necessary (Willoughby et al., 1987; Faull et al., 1993; Saydoff et al., 1996; Bealer and Crowley, 1998).

Hence, because enhanced AVP and OT release in the case of hormone demand is linked to increased peptide synthesis in the magnocellular neurons and because noradrenaline (NA) and serotonin (5-HT) stimulate AVP and OT release, we hypothesize that these monoamines could also modulate AVP and OT expression in the PVN and SON.

To test this hypothesis, we used a transgenic mouse model (Tg8), descending from C3H/HeJ, in which the inactivation of the monoamine oxidase-A (MAO-A) gene results in increased amounts of 5-HT and NA, but not of dopamine, in the brain (Cases et al., 1995). We analyzed the effect of chronic increased amounts of 5-HT and NA on AVP and OT expression in the PVN and SON by comparing peptide and mRNA levels in C3H and Tg8 adult mice, combining immunohistochemistry, enzyme immunoassays (EIA), and *in situ* hybridization. The respective contribution of 5-HT and NA to AVP and OT expression was

investigated in Tg8 mice by inhibiting catecholamine or 5-HT synthesis with α-methylparatyrosine (α-MPT) or parachlorophenylalanine (pCPA), respectively.

MATERIALS AND METHODS

Animals

All of the experiments were performed according to French and European legal requirements (Decree 87-848). Animals were killed at postnatal day 90, when 5-HT and NA concentrations are, respectively, 1.5- and twofold higher than in C3H mice (Cases et al., 1995). The 21 C3H/HeJ and 85 Tg8 mice used in this study were housed under a 12 hr light/dark cycle (lights on at 7 A.M.) with access to food and water *ad libitum*. They were always killed at the same time of the day (7–9 hr after lights on).

Pharmacological treatments

Three-month-old Tg8 mice were injected intraperitoneally once daily at 11 A.M. on 3 successive days with α-MPT methyl ester or pCPA methyl ester (300 mg/kg; concentration, 40 mg/ml in saline; Sigma, Lyon, France) or vehicle. Control Tg8 mice received a similar volume (depending on the weight) of saline solution only, according to the same schedule. C3H and Tg8 mice (control and treated) were killed between 3 and 5 hr after the last injection.

Serotonin, arginine-vasopressin, and oxytocin immunohistochemistry

Five C3H mice and 16 Tg8 mice (comprising 4 control, 4 saline-control, 4 α-MPT-treated, and 4 pCPA-treated Tg8 mice) were treated for immunohistochemistry. Animals were anesthetized with sodium pentobarbital (25 mg/kg) and perfused through the left ventricle with 50 ml of saline, followed by 50 ml of 4% paraformaldehyde in 0.1 M phosphate buffer, pH 7.4. Brains were removed, post-fixed in the same fixative for 4 hr at 4°C, and cryoprotected in 20% sucrose. Serial coronal 18-μm-thick sections were cut on a cryostat at −21°C. They were rinsed in 0.05 M PBS, pH 7.4, containing 1% bovine serum albumin (BSA) and 0.1% Triton X-100 for 2 hr at room temperature and were incubated overnight at 4°C with rabbit antisera against AVP or OT (1:4000; gift from Dr. G. Alonso) (Alonso, 1988) or 5-HT (1:2000; gift from Dr. Y. Tillet) (Tillet et al., 1986). Then the sections were rinsed three times for 10 min in PBS/BSA before detection of bound primary antibody via the avidin–biotin complex (ABC) system (Vector Laboratories, Peterborough, UK). The sections were incubated first for 1 hr at room temperature with biotinylated anti-rabbit IgG antibody (1:200 in PBS) and then for 1 hr at room temperature with peroxidase-labeled ABC (1:100 avidin and 1:100 biotin). After being rinsed in several baths of PBS, the peroxidase activity was developed by incubating the sections in 0.05 M Tris, pH 7.5, containing 0.05% 3,3'-diaminobenzidine (Sigma) and 0.006% H_2O_2 (Sigma). Finally, the sections were mounted in Permount for observation under a light microscope (Leitz, Wetzlar, Germany). Control experiments were performed by omitting primary or secondary antibodies.

Noradrenaline immunohistochemistry

Three C3H mice and nine Tg8 mice (3 control, 3 saline-control, and 3 α-MPT-treated) were used for the immunohistochemical detection of NA. After deep anesthesia with sodium pentobarbital (25 mg/kg), the animals were perfused with 50 ml of saline containing 1% sodium disulfite (SMD; Prolabo, Paris, France), followed by 80 ml of 2.5% glutaraldehyde in 0.1 M phosphate buffer, pH 7.4, containing 1% SMD. The brains were removed, post-fixed in the same fixative for 1 hr at 4°C, and cut coronally with a vibratome (Leica, Nussloch, Germany). Sections 50 μm thick were collected in 0.1 M PBS containing 1% SMD before being rinsed for 10 min in 0.1 M PBS containing 1% H_2O_2. Then they were washed for 5 min at room temperature in 0.1 M PBS containing 0.1% glycine and for 1 hr at room temperature in 0.1 M PBS containing 3% BSA, 1% SMD, and 0.2% saponin; finally, they were incubated overnight at 4°C with rabbit anti-NA antiserum (1:2000; gift from Dr. Y. Tillet) (Tillet et al., 1990). After a 30 min rinse in 0.1 M PBS containing 1.5% BSA, 1% SMD, and 0.2% saponin, bound primary antibody was detected by using the ABC system and 3,3'-diaminobenzidine (see above). Control experiments were performed as described above.

Arginine-vasopressin and oxytocin enzyme immunoassay

Peptide extraction. Nine C3H and 44 Tg8 mice (comprising 11 control, 11 saline-control, 11 α-MPT-treated, and 11 pCPA-treated Tg8 mice) were

used for EIA. Immediately after decapitation the brains were removed, frozen at −30°C in isopentane, and stored at −80°C. Thick sections (250 μm) were prepared via a cryostat at −18°C. The bilateral PVN and SON were punched out at −18°C under a magnifying glass by using a 200 μm internal diameter needle and stored at −80°C. For peptide extraction the PVN and SON were immersed separately in 100 μl of 0.01 M phosphate buffer, pH 7.4, and sonicated for 10 sec. Ten microliters were removed for the protein assay. After the addition of 90 μl of 4 M acetate, the samples were heated for 10 min at 95°C and centrifuged for 50 min at 13,000 rpm at 4°C. The supernatants were dried in a speed vacuum, and the dry residues were dissolved in EIA buffer (0.1 M potassium buffer, pH 7.4, 0.15 M NaCl, 0.1% BSA, and 0.01% sodium azide). AVP and OT were assessed in the same bilateral PVN or SON, and the protein concentration of each sample was determined by using the Coomassie Plus Protein Assay Reagent Kit (Pierce, Bezons, France).

Competitive enzyme immunoassay procedure. AVP and OT contents were measured by enzymatic competitive immunoassays (Pradelles et al., 1985). AVP and OT were obtained from Sigma. Enzymatic tracers were prepared by covalently coupling the peptide to acetylcholinesterase (AChE), using the heterobifunctional reagent *N*-succinimidyl-4 (*N*-maleimidomethyl) cyclohexane 1-carboxylate (SMCC), as described previously (McLaughlin et al., 1987). This method involves the reaction of thiol groups, previously introduced into peptides, with maleimido groups incorporated into the enzyme.

The rabbit anti-AVP and anti-OT antisera previously used in the immunohistochemistry experiments were diluted 1:50,000 and 1:10,000, respectively. A solid phase EIA was performed in 96-well microtiter plates (Immunoplate Maxisorp; Nunc, Roskilde, Denmark) coated with mouse monoclonal anti-rabbit IgG antibodies to ensure the separation of bound and free moieties of the enzymatic tracer during the immunological reaction. Fifty microliters of each of the fluid phase reactants peptide standard or sample, enzymatic tracer, and diluted rabbit antiserum were added to the plates, which then were incubated for 18 hr at 4°C and washed with 0.01 M phosphate buffer, pH 7.4, containing 0.05% Tween 20; the enzymatic activity of the solid phase bound immunological complex was revealed by the addition of Ellman's medium. After a 1.5 hr reaction at room temperature the absorbance of each well was measured at 414 nm. The sensitivity of the assay, measured as the concentration of unlabeled peptide inducing a 50% decrease in binding compared with that in the absence of competitor (B/Bo, 50%), was 750 pg/ml for AVP and 2 ng/ml for OT. The AVP and OT concentrations in the samples were calculated from the standard curves and standardized to the amount of protein.

In situ *hybridization of arginine-vasopressin and oxytocin mRNAs*

Probes. The probe used for the detection of AVP mRNA was 5'-TAC CAG CCT AAG CAG CAG CTC CCG GGC TGG CCC GTC CAG C-3', whereas that used for the detection of OT mRNA was 5'-CTC GGA GAA GGC AGA CTC AGG GTC G-3'. These probes have been used previously for the detection of AVP mRNA and OT mRNA in the rat hypothalamus by Trembleau et al. (1993) and Kawata et al. (1988). The specificity of both probes for the corresponding mouse mRNAs was verified by checking the DNA Database of Japan.

Probe labeling. The probes were 3'-end labeled with [^{35}S]dATP (>1000 Ci/mmol; Amersham, Bucks, UK), using terminal transferase (Boehringer Mannheim, Mannheim, Germany). Oligonucleotides (2 pmol) were incubated for 45 min at 37°C in a total volume of 10 μl containing 20 μCi of [^{35}S]dATP, 25 U of terminal transferase, 1 μl of 25 mM CoCl$_2$ (Boehringer Mannheim), 2 μl of 5× terminal transferase labeling buffer (1 M potassium cacodylate, 125 mM Tris-HCl, 1.25 mg/ml BSA, pH 6.6; Boehringer Mannheim), and 3 μl of sterile water; then the labeling reaction was stopped by the addition of 1 μl of a solution containing 0.2 M EDTA and 5 μg/μl tRNA (Sigma). Finally, 75 μl of cold absolute ethanol and 2.5 μl of 4 M LiCl were added, and the labeled probes were precipitated by overnight incubation at −20°C, followed by centrifugation (13,000 rpm) for 30 min at 4°C. The pellet, dried in a speed vacuum, was dissolved in 100 μl of 1 mM Tris base and 0.16 mM EDTA buffer, pH 8. The percentage of radioactivity that was incorporated, determined by counting the radioactivity in 5 μl of the pellet and 5 μl of the supernatant, was between 76 and 89%.

Hybridization procedures. Four C3H mice and 16 Tg8 mice (comprising 4 control, 4 saline-control, 4 α-MPT-treated, and 4 pCPA-treated Tg8 mice) were used for *in situ* hybridization. The tissues were prepared by using the same procedure as for immunohistochemistry except that the

fixative solution contained 1% paraformaldehyde, and sterile SuperFrost slides (Menzel Glaser, Frankfort, Germany) were used instead of gelatin-coated slides for mounting the brain sections. Brain sections were dehydrated in graded ethanol, delipidated in chloroform for 5 min, and rehydrated in reverse ethanol. Sections were hybridized directly overnight at 42°C with a 1 nM concentration of the radiolabeled AVP and OT probes diluted in hybridization buffer (50% formamide, 600 mM NaCl, 80 mM Tris-HCl, pH 7.5, 4 mM EDTA, 0.05% disodium pyrophosphate, 0.05% tetrasodium pyrophosphate, 0.2% N-lauryl sarcosyl, and 10 mM dithiothreitol; Sigma). Finally, the sections were washed four times for 15 min at 55°C in 1× SSC (0.15 M NaCl and 0.015 M trisodium citrate), followed by a final wash for 1 hr at room temperature in 0.1× SSC. Reaction specificity was confirmed by performing two kinds of control, omitting the probe or using an excess of unlabeled probes.

Detection of the ^{35}S-labeled oligonucleotides. The sections were dehydrated and placed in contact with Amersham-β-Max radiographic film (Amersham, Les Ulis, France) for 6 d at 4°C. Then the films were developed with Microdol X-Pro (Kodak, Rochester, NY), fixed in 25% Max-Fix (Kodak), and processed for the semiquantitative analysis. The slides were dipped in 50% Ilford nuclear emulsion (50% water) at 37°C, air-dried overnight, and exposed in the dark for 3 weeks at 4°C; finally, they were developed in Kodak D19 for 4 min at 18°C, rinsed in water, fixed in 30% sodium thiosulfate containing 0.05% aluminum potassium sulfate, washed in water, and mounted with Permount for light microscopy.

Statistical analysis

Data for the quantification of enzyme immunoassays and radioautograms are represented as the mean percentage of the control ± SEM. Results for different groups of mice were compared by one-way ANOVA, followed by a Scheffé's test, and were considered significant if $p < 0.05$.

RESULTS

Effects of monoamine oxidase-A gene inactivation on arginine-vasopressin expression in the paraventricular and supraoptic nuclei

Arginine-vasopressin expression

In C3H mice the AVP-immunoreactive (AVP-IR) neurons were located primarily in the medial portion of the PVN (Fig. 1A) and occupied the major part of the SON (Fig. 1E). We could not distinguish the parvocellular and the magnocellular portions of the PVN. Numerous AVP-IR processes, identified as axons, left the PVN and headed laterally and ventrally for the SON. In Tg8 mice the AVP-IR perikarya were stained more intensely in the PVN (Fig. 1B) as well as in the SON (Fig. 1F) than in C3H mice (Fig. 1A,E). This increase in staining seemed to concern the totality of AVP-IR neurons in the PVN. The axons leaving the PVN were stained more strongly for AVP in Tg8 mice compared with C3H mice. EIA of the paraventricular and supraoptic AVP contents showed a significant 107% ($p < 0.05$) increase in the PVN (see Fig. 7A) and a significant but more moderate 33% ($p < 0.05$) increase in the SON of Tg8 mice compared with C3H mice (see Fig. 7C).
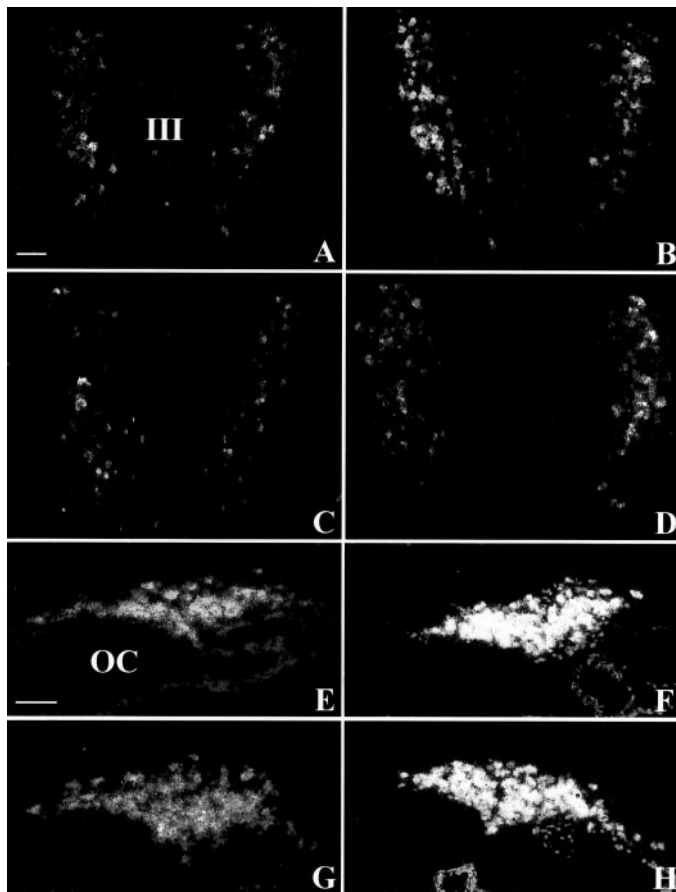
In control C3H mice the hybridization signal of AVP mRNA obtained on emulsion-coated sections was concentrated in the medial PVN (Fig. 2A) and in an extended ventral portion of the SON (Fig. 2E). In Tg8 mice the distribution of silver grains on emulsion-dipped sections was not more extended in the PVN (Fig. 2B) nor in the SON (Fig. 2F). However, each stained cell body presented an increased density of silver grains. This increase concerned all of the perikarya and did not favor any subdivision of the PVN. Quantitation by densitometry on films estimated the enhanced hybridization signal for AVP mRNA in Tg8 mice as 98% (significant with $p < 0.01$; see Fig. 7B) in the PVN and as 130% (significant with $p < 0.05$; see Fig. 7D) in the SON of C3H mice.
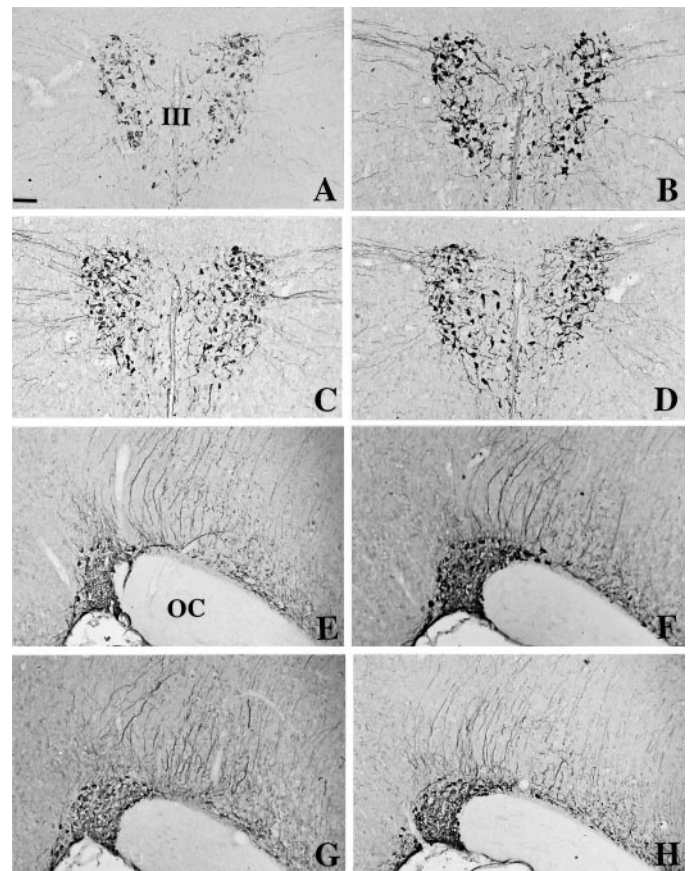
Figure 1. Immunohistochemical detection of arginine-vasopressin in the PVN (*A–D*) and in the SON (*E–H*) of C3H mice (*A, E*), Tg8 mice (*B, F*), α-MPT-treated Tg8 mice (*C, G*), and pCPA-treated Tg8 mice (*D, H*). The mutation is associated with an increase in AVP immunoreactivity in the PVN (*B* vs *A*) and in the SON (*F* vs *E*). No difference was observed between Tg8 and saline-control Tg8 mice. The treatment by α-MPT in Tg8 mice is correlated with a decline in AVP immunoreactivity in the PVN (*C*) as well as in the SON (*G*) compared with saline-control Tg8 mice (the same as *B, F*). In pCPA-treated Tg8 mice the intensity of labeling is also decreased in the PVN (*D*) and in the SON (*H*) compared with saline-control Tg8 mice. *III*, Third ventricle; *OC*, optic chiasma. Scale bar, 50 μm.

Oxytocin expression

In C3H mice the OT-immunoreactive (OT-IR) cell bodies were located primarily in the peripheral PVN (Fig. 3A) and occupied the dorsal portion of the SON (Fig. 3E). They were more scattered than AVP-IR neurons in the PVN as well as in the SON. Moreover, they were less numerous than AVP-IR in the SON (~10 cell bodies per section). Two kinds of OT-IR fibers were observed: long fibers emerging from the PVN and descending toward the SON, and shorter processes limited to the PVN and SON. The immunoperoxidase signal was increased in intensity and in the number of OT-IR neurons both in the PVN and SON in Tg8 mice (Fig. 3B,F, respectively, compared with *A,E*) compared with C3H mice. The augmentation of immunoreactivity affected all of the OT-positive cells. Fibers were also stained more intensely for OT in the PVN and SON of Tg8 mice compared with C3H mice. Moreover, OT-immunopositive perikarya appeared to be larger in Tg8 mice, particularly in the SON. Using EIA to quantify OT, we estimated the augmentation of the OT level as 66% (significant with $p < 0.05$) in the PVN (see Fig. 8A)

Figure 2. Dark-field microphotographs representing the *in situ* hybridization signal of AVP mRNA on emulsion-coated sections in C3H mice (*A, E*), Tg8 mice (*B, F*), α-MPT-treated Tg8 mice (*C, G*), and pCPA-treated Tg8 mice (*D, H*). Compared with C3H mice (*A, E*), the hybridization signal is increased but distributed similarly both in the PVN (*B*) and the SON (*F*) in Tg8 mice. No difference was detected between Tg8 mice and saline-control Tg8 mice. In α-MPT-treated Tg8 mice the hybridization signal is decreased in the PVN (*C*) as well as in the SON (*G*) compared with saline-control Tg8 mice (the same as *B, F*). In pCPA-treated Tg8 mice the density of silver grains is decreased in the PVN (*D*) compared with saline-control Tg8 mice. In contrast, no difference is observed between pCPA-treated Tg8 mice and saline-control Tg8 in the SON (*G*). *III*, Third ventricle; *OC*, optic chiasma. Scale bars, 50 μm.
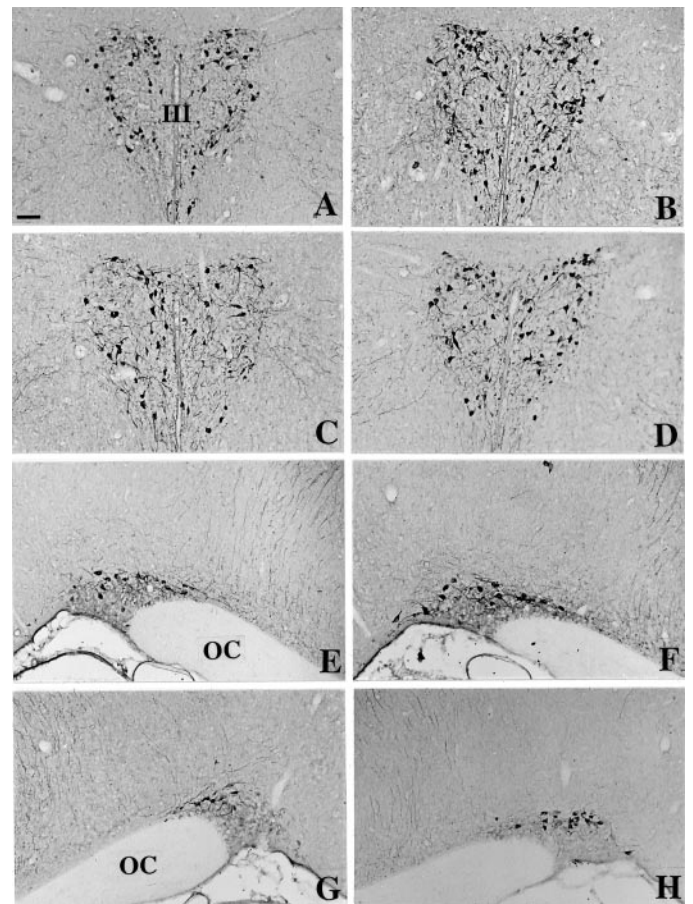
Figure 3. Immunohistochemical detection of oxytocin in the PVN (*A–D*) and in the SON (*E–H*) of C3H mice (*A, E*), Tg8 mice (*B, F*), α-MPT-treated Tg8 mice (*C, G*), and pCPA-treated Tg8 mice (*D, H*). Compared with C3H mice, OT-immunostained neurons are stained more strongly and are more numerous in Tg8 mice both in the PVN (*B*) and the SON (*E*). In α-MPT-treated Tg8 mice the intensity of OT immunoreactivity as well as the number of OT-immunopositive neurons declines in the PVN (*C*) and in the SON (*G*) compared with saline-control Tg8 mice (the same as *B, F*). Likewise, the treatment by pCPA in Tg8 mice is associated with a decrease in the number of OT-immunostained cell bodies and in the intensity of OT labeling both in the PVN (*D*) and the SON (*H*) compared with saline-control Tg8 mice. *III*, Third ventricle; *OC*, optic chiasma. Scale bar, 50 μm.

and as 123% (significant with $p < 0.05$) in the SON (see Fig. 8*C*) of Tg8 mice versus C3H mice.

In control C3H mice the distribution of the OT mRNA radioactive signal on emulsion-coated sections corresponded to the immunohistochemical signal both in the PVN (Fig. 4*A*) and in the SON (Fig. 4*E*). The cellular density of silver grains was greater in Tg8 mice than in C3H mice in the PVN (Fig. 4*B* related to *A*) and in the SON (Fig. 4*F* vs *E*). This increase concerned the totality of the stained cell bodies. Densitometry quantitation on radioautograms revealed a significant 48% augmentation ($p < 0.05$) in the PVN (see Fig. 8*B*) and a significant 83% increase ($p < 0.05$) in the SON (see Fig. 8*D*) of the radioactive signal for OT mRNA in Tg8 mice compared with C3H ones.

Effects of monoamine oxidase-A gene inactivation on noradrenaline and serotonin immunoreactivities in the paraventricular and supraoptic nuclei

Noradrenaline immunoreactivity

In control C3H mice the NA immunoreactivity was intense in the PVN (Fig. 5*A*). Numerous NA-IR fibers and varicosities were

observed throughout the nucleus. Immunopositive varicosities surrounded immunonegative cell bodies. Moreover, some processes were detected laterally, outside the PVN. In Tg8 mice the NA-IR varicosities were more abundant and labeled more intensely, compared with C3H mice, throughout the brain and notably in the PVN (compare Fig. 5*B,A*). This increase in NA immunoreactivity was pronounced particularly in the dorsolateral portion of the nucleus. The considerable volume and density of varicosities surrounding immunonegative perikarya resulted in an opaque appearance of the cytoplasm in cell bodies.

For SON, in control C3H mice the NA-IR fibers and varicosities surrounded immunonegative perikarya throughout the supraoptic mass without any regional differences (Fig. 5*D*). Moreover, some NA-immunostained fibers were also detected immediately above the SON. Immunonegative cell bodies were surrounded by varicosities (*arrow*). In Tg8 mice the NA-immunostained processes and varicosities were more abundant and stained more intensely than in C3H mice (compare Fig.
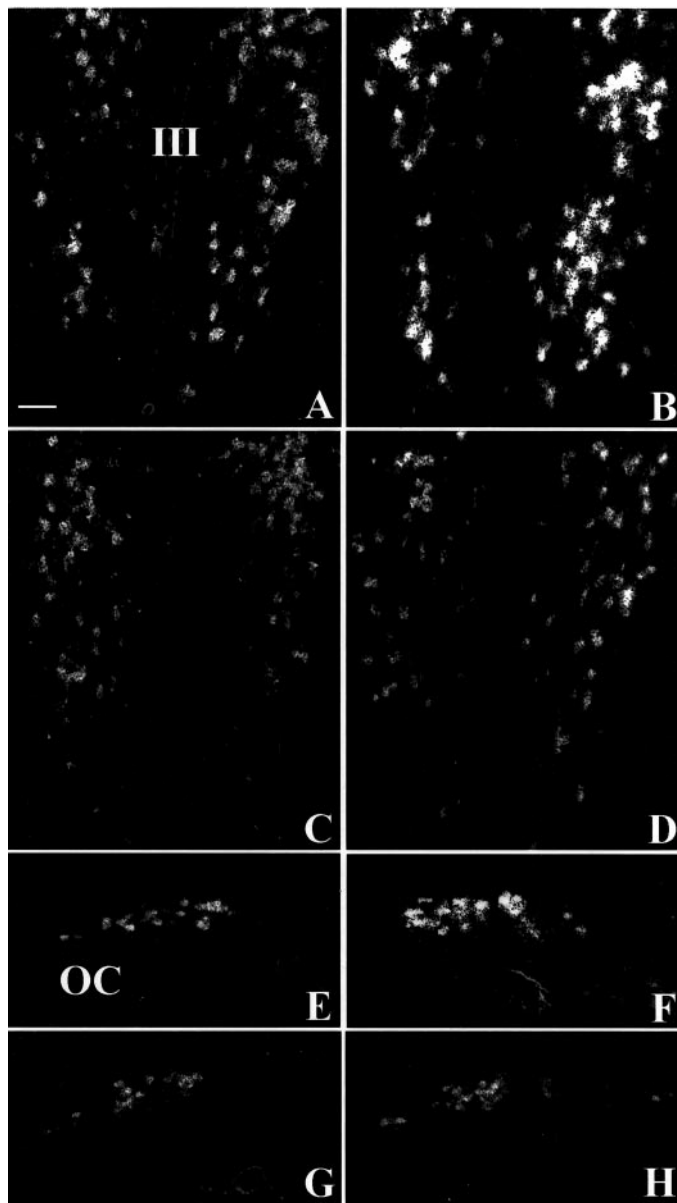
Figure 4. Dark-field microphotographs representing the *in situ* hybridization signal of OT mRNA on emulsion-coated sections in C3H mice (*A, E*), Tg8 mice (*B, F*), α-MPT-treated Tg8 mice (*C, G*), and pCPA-treated Tg8 mice (*D, H*). The hybridization signal is enhanced in Tg8 mice both in the PVN (*B*) and the SON (*F*) compared with C3H mice (*A, E*). In α-MPT-treated Tg8 mice the hybridization signal is reduced in the PVN (*C*) as well as in the SON (*G*) compared with saline-control Tg8 mice (the same as *B, F*). In pCPA-treated Tg8 mice the density of silver grains is also decreased in the PVN (*D*) and in the SON (*G*) compared with saline-control Tg8 mice. *III*, Third ventricle; *OC*, optic chiasma. Scale bar, 50 μm.

5*E,D*). The high density of stained varicosities surrounding the unstained cell bodies (*arrow*) rendered the entire SON opaque to photons.

Serotonin immunoreactivity

5-HT immunoreactivity was weak in the PVN compared with the other brain regions. In wild-type mice the scarce fibers presented varicosities surrounding immunonegative cell bodies (Fig. 6*A, arrow*). They were distributed homogeneously throughout the PVN. In Tg8 mice the 5-HT-IR fibers and varicosities were more

abundant in the PVN (Fig. 6*B*) as well as in the whole brain, compared with C3H mice (Fig. 6*A*). Moreover, varicosities surrounding unstained perikarya (*arrow*) appeared to be larger and more intensely stained.

In C3H mice the 5-HT-IR fibers and varicosities were quite rare in the SON (Fig. 6*D*). 5-HT-immunostained fibers were distributed preferentially around the SON. In the SON of Tg8 mice the 5-HT-IR processes and varicosities were more numerous and surrounded unstained perikarya (Fig. 6*E, arrow*), predominantly in the ventral portion of the nucleus.

Pharmacology: Respective involvement of serotonin and noradrenaline in arginine-vasopressin and oxytocin expression

All of the morphological and semiquantitative data obtained for Tg8 mice (NA, 5-HT, AVP, and OT) were unchanged with intraperitoneal injections of an NaCl solution. Consequently, microphotographs and quantitations corresponding to the non-injected Tg8 phenotype are taken as references to compare treated Tg8 mice with saline-control Tg8 ones.

Effect of α-methylparatyrosine administration

The intensity of AVP immunoreactivity was depressed strongly within all of the cell bodies, but not in fibers in α-MPT-treated Tg8 mice compared with saline-control Tg8 ones both in the PVN (Fig. 1*C* vs *B*) and in the SON (Fig. 1*G* related to *F*). Moreover, the size of perikarya seemed to be decreased. EIA evaluated the decrease in AVP content in α-MPT-treated Tg8 mice as 52% ($p < 0.05$) in the PVN (Fig. 7*A*) and as 77% ($p < 0.001$) in the SON (Fig. 7*C*) in comparison with saline-control Tg8 mice. In α-MPT-treated Tg8 mice the AVP mRNA radioactive signal was decreased compared with that in saline-control Tg8 mice both in the PVN (compare Fig. 2*C,B*) and in the SON (Fig. 2*G* vs *F*). After administration of α-MPT the silver grains on emulsion-dipped sections corresponded to a similar region in saline-control Tg8 mice, but their density was greatly reduced. Levels of radioactivity quantified on films were reduced by 41% ($p < 0.05$) compared with saline-control Tg8 mice in the PVN (Fig. 7*B*) and by 58% ($p < 0.05$) compared with saline-control Tg8 mice in the SON (Fig. 7*D*).

In comparison with saline-control Tg8 mice, α-MPT-treated Tg8 mice presented a decrease in the number of OT-stained perikarya both in the PVN and SON. Some neurons were as immunopositive as in saline-control Tg8 mice, whereas others, particularly in the central portion of the PVN, exhibited a profound depression in OT immunoreactivity (compare Fig. 3*C,B*). The appearance of the fibers remained unchanged in the PVN of α-MPT-treated Tg8 mice compared with saline-control Tg8 mice. In the SON α-MPT treatment was associated with a decline in the number of strongly stained OT-IR neurons (Fig. 3*G* related to *F*). Both neurons and fibers were less stained after the treatment. Moreover, OT-immunopositive perikarya appeared to be smaller in α-MPT-treated Tg8 compared with saline-control Tg8 mice in the SON. In the α-MPT-treated group OT amounts determined by EIA were reduced by 33% ($p < 0.05$) in the PVN (Fig. 8*A*) and by 67% ($p < 0.001$) in the SON (Fig. 8*C*) compared with saline-control Tg8 mice. The administration of α-MPT to Tg8 mice was also associated with a decrease in the intensity of the OT mRNA hybridization signal compared with saline-control Tg8 mice both in the PVN and the SON. On emulsion-coated sections the distribution of silver grains in the PVN in catecholamine-depleted Tg8 mice was similar to that in saline-
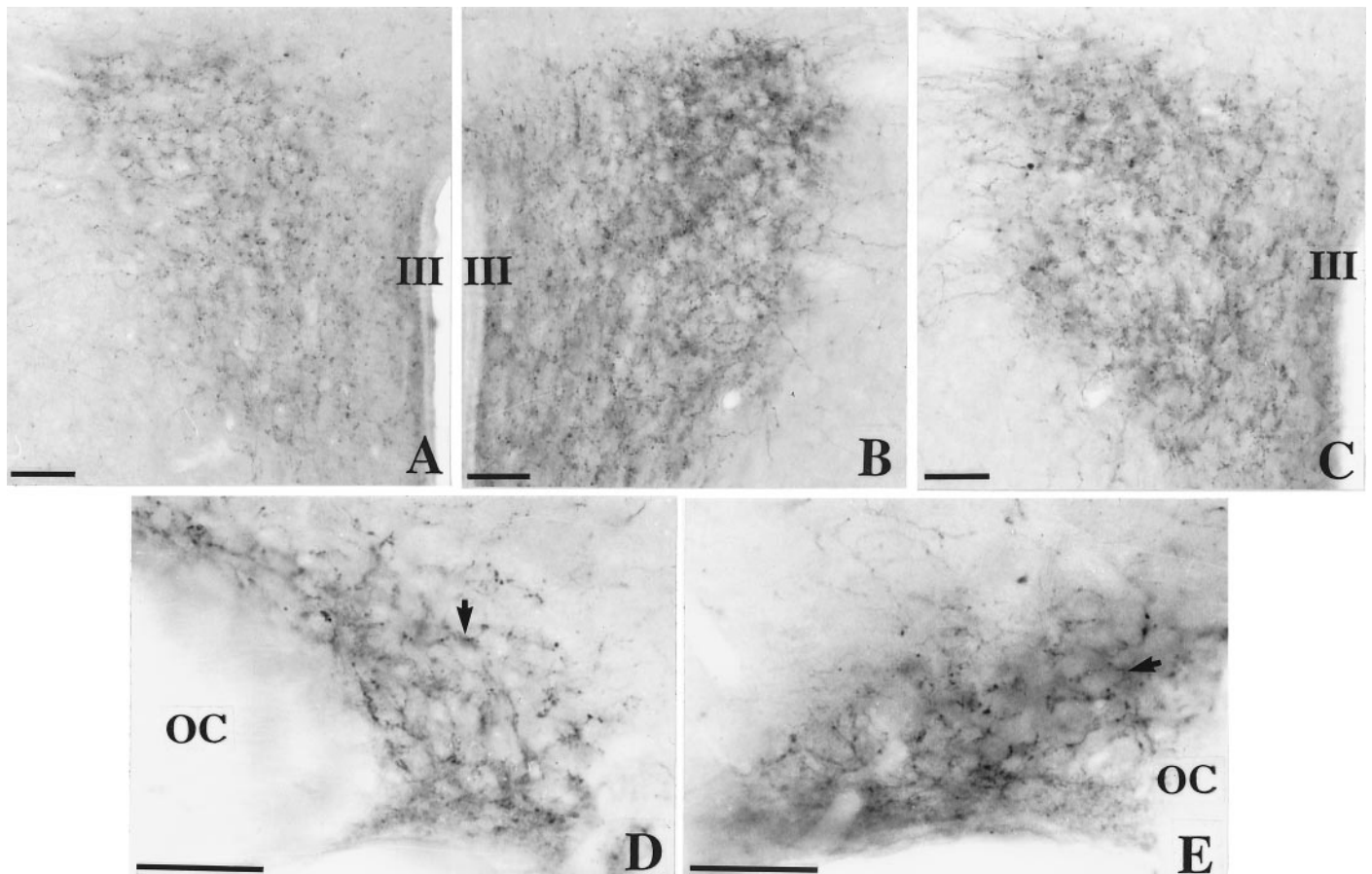
Figure 5. Immunohistochemical detection of noradrenaline in the PVN (*A–C*) and in the SON (*D, E*) of C3H mice (*A, D*), Tg8 mice (*B, E*), and α-MPT-treated Tg8 mice (*C*). Compared with C3H mice (*A*), both the density of immunostained fibers and the staining intensity are increased in the PVN in Tg8 mice (*B*). Likewise, the labeling intensity of varicosities surrounding unstained cell bodies is enhanced in the SON of Tg8 mice (*arrow, E*) compared with C3H mice (*D*). With the treatment of Tg8 mice by α-MPT, the intensity of NA immunostaining declined in the PVN (*C*) in comparison with saline-control Tg8 mice (the same as *B*). *III*, Third ventricle; *OC*, optic chiasma. Scale bars, 50 μm.

control Tg8 mice, but radioautographic labeling was less intense (compare Fig. 4*C,B*). In the SON, cell bodies that were overlapped by the hybridization signal were less numerous and less stained in the α-MPT-treated Tg8 mice compared with saline-control Tg8 mice (Fig. 4*G* vs *F*). Quantitation by densitometry on films showed a significant decline in radioactivity of 42% ($p <$ 0.001) in the PVN (Fig. 8*B*) and of 50% ($p <$ 0.01) in the SON (Fig. 8*D*) in comparison with saline-control Tg8 mice.

Administration of α-MPT to Tg8 mice was associated with a decline in the intensity of NA immunostaining in the PVN and the SON of Tg8 mice compared with saline-control Tg8 mice. In the PVN the NA-IR fibers and varicosities were stained less intensely in α-MPT-treated Tg8 mice (Fig. 5*C*) compared with saline-control Tg8 mice (Fig. 5*B*), but their number seemed to be unchanged after the treatment. In the SON of α-MPT-treated Tg8 mice the NA-IR fibers and varicosities were stained less intensely compared with saline-control Tg8 mice (data not shown). The size of varicosities appeared to be reduced with the treatment.

Effect of parachlorophenylalanine administration
The treatment by pCPA was associated with a decline in intensity for the AVP immunostaining, but not in the number of AVP-IR neurons in the PVN (Fig. 1*D* related to *B*) or in the SON (Fig. 1*H* vs *F*). However, AVP immunoreactivity in fibers was not different

in 5-HT-depleted mice compared with saline-control Tg8 mice. EIA of AVP contents in pCPA-treated Tg8 mice revealed a significant decrease of 57% ($p <$ 0.01) in the PVN (Fig. 7*A*) and of 63% ($p <$ 0.001) in the SON (Fig. 7*C*) in comparison with saline-control Tg8 mice. In the PVN the AVP mRNA hybridization signal was less intense in pCPA-treated Tg8 mice (Fig. 2*D*) in comparison with saline-control Tg8 mice (Fig. 2*B*). On emulsion-dipped sections the silver grains seemed to be less abundant per cell body with pCPA-treatment, but the number of perikarya exhibiting a radioactive signal remained the same compared with saline-control Tg8 mice. Nevertheless, the radioactive signal of AVP mRNA in the SON was similar in pCPA-treated Tg8 mice and in saline-control Tg8 mice (Fig. 2*H* vs *F*). Quantitation by densitometry on films showed a significant reduction in radioactivity in the PVN of pCPA-treated Tg8 mice of 34% ($p <$ 0.05) compared with saline-control Tg8 ones (Fig. 7*B*), whereas no significant difference was evaluated in the SON between pCPA-treated and saline-control Tg8 mice (Fig. 7*D*).

Administration of pCPA was associated with a decrease in the intensity of OT immunoreactivity and in the number of OT-IR neurons compared with saline-control Tg8 mice in the PVN (Fig. 3*D* related to *B*). In the SON the intensity of staining and the size of OT-IR perikarya were decreased, whereas the number of OT-immunostained neurons remained unchanged in pCPA-
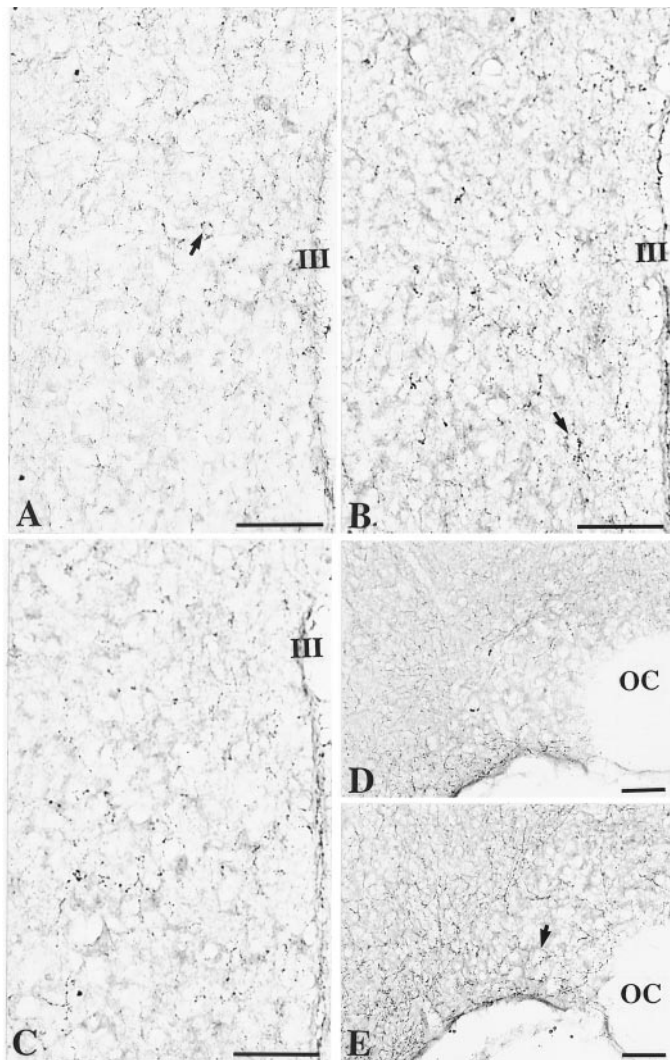
Figure 6. Immunohistochemical detection of serotonin in the PVN (*A–C*) and in the SON (*D, E*) of C3H mice (*A, D*), Tg8 mice (*B, E*), and pCPA-treated Tg8 mice (*C*). In Tg8 mice the density of 5-HT-positive varicosities surrounding unstained cell bodies and the labeling intensity are increased in the PVN (*A, B, E, arrow*) compared with C3H mice (*A*). In the SON of Tg8 mice the number of 5-HT-immunopositive fibers increases, particularly in the ventral portion of the nucleus (*E*), compared with C3H mice (*D*). Treatment by pCPA in Tg8 mice induces a decrease in the density of 5-HT-immunostained varicosities in the PVN (*C*) compared with saline-control Tg8 mice (the same as *B*). *III*, Third ventricle; *OC*, optic chiasma. Scale bars, 50 μm.

treated Tg8 in comparison with saline-control Tg8 mice (compare Fig. 3*H,F*). In pCPA-treated Tg8 mice the OT amounts determined by EIA decreased by 38% ($p < 0.05$) in the PVN (Fig. 8*A*) and by 55% ($p < 0.05$) in the SON (Fig. 8*C*) compared with saline-control Tg8 mice. In pCPA-treated Tg8 mice the OT mRNA hybridization signal on emulsion-coated sections was less intense but equally extended as in saline-control Tg8 mice in the PVN (Fig. 4*D* vs *B*). In contrast, in the SON the administration of pCPA was associated with a decrease in the number of stained perikarya as well as in the staining intensity (compare Fig. 4*H,F*). In the quantification of optical density on radioautograms, the hybridization signal was decreased significantly by 44% ($p < 0.05$) in the PVN (Fig. 8*B*) and by 43% ($p < 0.05$) in the SON (Fig. 8*D*) compared with saline-control Tg8 mice.

In pCPA-treated Tg8 mice the 5-HT immunoreactivity was decreased both in the PVN and SON compared with saline-control Tg8 mice. In the PVN (Fig. 6*C*) the density of immuno-labeled fibers and varicosities, as well as the staining intensity, appeared to be lower after the pCPA treatment compared with saline-control Tg8 mice (Fig. 6*B*). However, the size of varicosities in pCPA-treated Tg8 mice looked higher than in C3H mice. In the SON of pCPA-treated Tg8 mice the 5-HT-IR fibers and varicosities seemed to be stained less intensely, but were not less numerous, than in saline-control Tg8 mice (data not shown).

DISCUSSION

In our study we demonstrate that the lack of MAO-A is associated with an increase in AVP and OT peptides and mRNA both in the PVN and SON. Peptide contents determined by immuno-histochemistry and EIA reflect the difference between the expression of the peptide and its axonal exportation for secretion. By coupling these methods with an analysis of mRNA levels by *in situ* hybridization, we can evaluate the expression parameter and so discriminate the effect of a factor on expression or on secretion. Considering (1) that magnocellular paraventricular and supraoptic neurons respond to several stimuli, such as osmotic ones, by increasing synthesis and release of AVP and OT and (2) that NA and 5-HT are to date only known to increase AVP and OT release in the systemic circulation, the aim of the present study was to inquire whether NA and 5-HT could also enhance AVP and OT expression in the PVN and SON. To test this hypothesis, we used a transgenic mouse model in which the inactivation of the gene encoding the MAO-A is responsible for specific increased amounts of NA and 5-HT, but not of dopamine, in the brain. AVP and OT expression was explored at the peptide and mRNA levels by coupling a qualitative analysis to a semiquantitative one.

In comparison with nontransgenic mice (C3H strain), the deficiency in MAO-A in Tg8 mice was correlated with an increase in brain NA-immunostaining intensity, which was marked particularly in the PVN and SON. This observation is in accordance with HPLC assays performed by Cases et al. (1995) on the whole brain. Several studies indicate that NA participates in the control of neuronal activity in the PVN and SON. For instance, the activation of magnocellular neurons in the PVN and SON after the stimulation of the A1/A2 cell groups is abolished by the destruction of noradrenergic inputs to the hypothalamus with 6-hydroxydopamine injection (Day and Renaud, 1984; Day et al., 1984; Tanaka et al., 1985; Kim et al., 1989). Consequently, we hypothesized that NA could be implicated in the modifications of AVP and OT expression in Tg8 mice. To test this hypothesis, we treated Tg8 mice with a catecholamine synthesis inhibitor, α-MPT. This treatment was associated with decreases in AVP and OT levels and in their mRNA in the PVN and SON. These results suggest a positive effect of NA on AVP and OT expression in the mouse PVN and SON. The discrepancy between our results and those of Itoi et al. (1999) showing that a local and acute NA injection into the PVN does not modify AVP mRNA levels significantly in the magnocellular portion of the nucleus could be related to the different experimental schedule. Indeed, in our transgenic model the levels of 5-HT and NA are elevated throughout the whole life of the animals, resulting in stable developmental modifications of the brain as suggested by Cases et al. (1996) and Beltramo et al. (1997). Moreover, the noradrener-gic control on AVP and OT neurons is strongly dependent on the delivery schedule of NA that is used, because NA dose-dependently stimulates different subtypes of adrenergic recep-
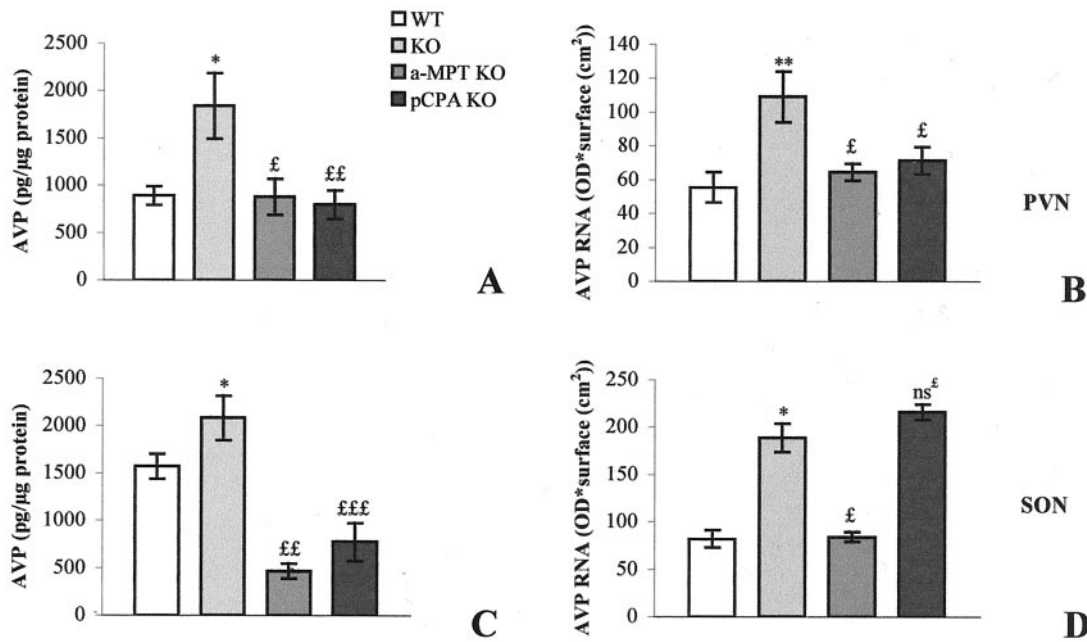
Figure 7. Enzyme immunoassay of AVP (*A, C*) and *in situ* hybridization of AVP mRNA (*B, D*) in the PVN (*A, B*) and the SON (*C, D*). Data are expressed as picograms of peptide/micrograms of protein (AVP level) or as optical density $\times$ surface (cm^2) (AVP mRNA) $\pm$ SEM; $*p < 0.05$ and $**p < 0.01$ compared with C3H mouse value with one-way ANOVA. $^£p < 0.05$; $^{££}p < 0.01$; $^{£££}p < 0.001$; ns $^£$, nonsignificant compared with saline-control Tg8 mouse value (which was equivalent to that of control Tg8 mice).
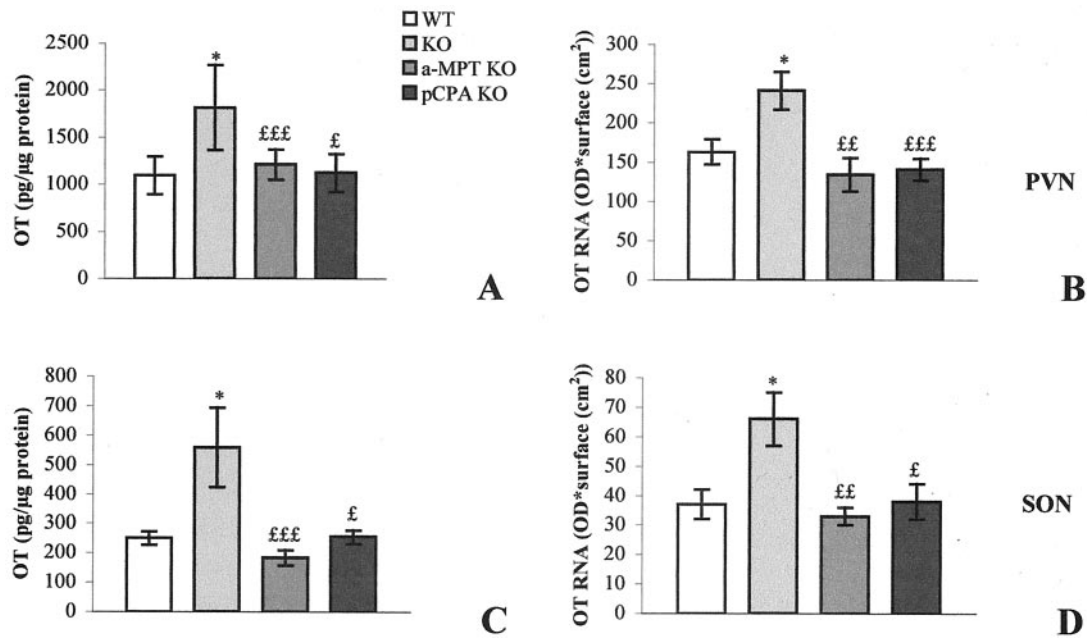

Figure 8. Enzyme immunoassay of OT (*A, C*) and *in situ* hybridization of OT mRNA (*B, D*) in the PVN (*A, B*) and the SON (*C, D*). Data are expressed as picograms of peptide/micrograms of protein (OT level) or as optical density $\times$ surface (cm^2) (AVP mRNA) $\pm$ SEM; $*p < 0.05$ compared with C3H mouse value, using one-way ANOVA. $^£p < 0.05$; $^{££}p < 0.01$; $^{£££}p < 0.001$ compared with saline-control Tg8 mouse value (which was equivalent to that of control Tg8 mice).

tors. Indeed, numerous studies indicate that NA stimulates AVP release via $\alpha 1$ receptors but inhibits AVP secretion via $\alpha 2$ and β receptors in the case of high NA doses (Day et al., 1985; Armstrong et al., 1986; Benetos et al., 1986; Brooks et al., 1986; Randle et al., 1986; Willoughby et al., 1987; Yamashita et al., 1987; Leibovitz et al., 1990; Shioda et al., 1997). Likewise, NA is suggested to mediate OT release during the reflex of suckling-

induced milk ejection and parturition but also to inhibit OT release, depending on the activated subtype of adrenergic receptor (Tribollet et al., 1978; Moos and Richard, 1979; Crowley et al., 1987; Song et al., 1988; Bealer and Crowley, 1998, 1999). In Tg8 mice, unpublished data of our laboratory indicate that the plasma concentration of AVP is increased because the hematocrit and water intake are decreased significantly compared with C3H

mice. Consequently, the fact that the augmentations of peptide contents followed those of mRNA in the PVN suggests either that NA could stimulate peptide expression rather than peptide secretion or that the hypervolemia revealed by the decreased hematocrit in Tg8 mice could weaken peptide release by the paraventricular neurons. In the SON the AVP level increased less than the AVP mRNA level. This could indicate either an action of NA on both the expression and the release of AVP or a limited retrocontrol of the AVP-induced hypervolemia on AVP release by the supraoptic neurons.

The 5-HT immunostaining in the PVN and SON of Tg8 mice indicates that the inactivation of MAO-A in Tg8 mice was associated with an increased amount of 5-HT in the brain (in accordance with the report of Cases et al., 1995). To clarify the possibility that 5-HT could, as well as NA, be partly responsible for increased expression of AVP and OT in the PVN and SON, we treated Tg8 mice with pCPA, a 5-HT synthesis inhibitor. This treatment induced in Tg8 mice a decrease in AVP and OT levels in the PVN and SON, which became similar to those in C3H mice. Moreover, compared with saline-control Tg8 mice, AVP and OT mRNA levels were also decreased in pCPA-treated Tg8 mice and restored to C3H levels in the PVN. However, in the SON the OT mRNA declined after pCPA treatment, whereas AVP mRNA remained similar in pCPA-treated Tg8 mice and in saline-control Tg8 mice. Consequently, it seems that 5-HT does not regulate AVP mRNA levels in the SON. Although the serotonergic input is moderate in the PVN and SON, several studies have demonstrated that 5-HT is able to modulate the activity of magnocellular AVP and OT neurons in these nuclei. The administration of D-fenfluramine, a 5-HT releaser and reuptake inhibitor, or fluoxetine, a 5-HT reuptake inhibitor, induces an increase in plasma AVP and OT levels (Saydoff et al., 1991; Faull et al., 1993), and this effect can be abolished by treating rats with pCPA (Iovino and Steardo, 1985). Nevertheless, the analysis of c-*fos* activation by D-fenfluramine injection indicates that the serotonergic input induces a c-*fos* transcription primarily in OT-containing neurons and quite moderately in AVP-ergic neurons in the PVN and SON, suggesting the existence of different regulation mechanisms by 5-HT in OT and AVP neurons (Mikkelsen et al., 1999), which is in accordance with our data.

Because variations in the paraventricular levels of AVP and OT were similar to those observed for mRNA in 5-HT-depletion conditions, we hypothesize that 5-HT could stimulate peptide expression without any noticeable effect on peptide release in this nucleus. However, the treatment with pCPA did not modify the AVP mRNA level in the SON of Tg8 mice although the AVP content was greatly reduced. These data could reveal an AVP translation positively regulated and/or an AVP release negatively regulated by 5-HT. The underlying mechanisms must be defined further, and multiple subtype receptors mediating these differential effects of 5-HT on AVP and OT contents in the PVN and SON could be suggested: 5-HT1A, 5-HT2A, and/or 5-HT2C (Bagdy, 1996; Saydoff et al., 1996; Vicentic et al., 1998).

Because we could not discriminate the parvocellular component in the PVN and because the modifications of AVP and OT levels, as well as of their mRNAs, seemed to concern the entire PVN, we suggest that NA and 5-HT also could activate AVP and OT expression in the parvocellular portion of the PVN. The stimulation of OT neurons in the parvocellular PVN by 5-HT has been suggested by a pharmacological study (Javed et al., 1999). In contrast, the implication of NA in such regulation is still debated (Alonso et al., 1986; Itoi et al., 1999) and is dependent on the

experimental schedule. However, we can hypothesize that, in our model, 5-HT and NA could participate in the regulation of the antehypophyseal release of ACTH concomitant with the increase in AVP and OT expression in parvocellular neurons observed after stressful stimuli (Plotsky, 1987) or during cardiac activity (Dreifuss et al., 1988) and penile erection (Giuliano and Rampin, 2000).

In conclusion, the current study demonstrates that NA and 5-HT, two monoamines known to control AVP and OT secretion from the neurohypophysis, are also involved in the regulation of these peptide expressions in the PVN and SON of the hypothalamus. We suggest that these regulations implicate complex mechanisms acting at the mRNA and/or peptide levels. These regulations taken as a whole may be involved in the restocking of hormones in the hypothalamus, offsetting their massive secretion, playing an important role in multiple functions such as extracellular fluid balance regulation, lactation, and parturition. Likewise, our study indicates that NA and 5-HT could also stimulate AVP and OT expression in the parvocellular PVN, suggesting a putative involvement of these monoamines in the triggering of ACTH secretion in response to stress and in the regulation of multiple vegetative functions such as penile erection and the modulation of cardiac frequency.

REFERENCES

Alonso G (1988) Effects of colchicine on the intraneuronal transport of secretory material prior to the axon: a morphofunctional study in hypothalamic neurosecretory neurons of the rat. Brain Res 453:191–203.

Alonso G, Szafarczyk A, Balmefrezol M, Assenmacher I (1986) Immunocytochemical evidence for stimulatory control by the ventral noradrenergic bundle of parvocellular neurons of the paraventricular nucleus secreting corticotropin-releasing hormone and vasopressin in rats. Brain Res 397:297–307.

Amaya F, Tanaka M, Tamada Y, Tanaka Y, Nilaver G, Ibata Y (1999) The influence of salt loading on vasopressin gene expression in magno- and parvocellular hypothalamic neurons: an immunocytochemical and *in situ* hybridization analysis. Neuroscience 89:515–523.

Armstrong WE, Gallagher MJ, Sladek CD (1986) Noradrenergic stimulation of supraoptic neuronal activity and vasopressin release *in vitro*: mediation by an α1 receptor. Brain Res 365:192–197.

Bagdy G (1996) Role of the hypothalamic paraventricular nucleus in 5-HT1A, 5-HT2A, and 5-HT2C receptor-mediated oxytocin, prolactin, and ACTH/corticosterone responses. Behav Brain Res 73:277–280.

Bealer SL, Crowley WR (1998) Noradrenergic controls of central oxytocin release during lactation in rats. Am J Physiol 274:E453–E458.

Bealer SL, Crowley WR (1999) Stimulation of central and systemic oxytocin release by histamine in the paraventricular hypothalamic nucleus: evidence for an interaction with norepinephrine. Endocrinology 140:1158–1164.

Beltramo M, Calas A, Chernigovskaya E, Thibault J, Ugrumov M (1997) Long-lasting effect of catecholamine deficiency on differentiating vasopressin and oxytocin neurons in the rat supraoptic nucleus. Neuroscience 79:555–561.

Benetos A, Gavras I, Gavras H (1986) Norepinephrine applied in the paraventricular hypothalamic nucleus stimulates vasopressin release. Brain Res 381:322–326.

Brooks DP, Share L, Crofton JT (1986) Central adrenergic control of vasopressin release. Neuroendocrinology 42:416–420.

Cases O, Seif I, Grimsby J, Gaspar P, Chen K, Pournin S, Müller U, Aguet M, Babinet C, Chen Shih J, de Maeyer E (1995) Aggressive behavior and altered amounts of brain serotonin and norepinephrine in mice lacking MAOA. Science 268:1763–1766.

Cases O, Vitalis T, Seif I, de Maeyer E, Sotelo C, Gaspar P (1996) Lack of barrels in the somatosensory cortex of monoamine oxidase A-deficient mice: role of a serotonin excess during the critical period. Neuron 16:297–307.

Crowley WR, Shyr SW, Kacsoh B, Grosvenor CE (1987) Evidence for stimulatory noradrenergic and inhibitory dopaminergic regulation of oxytocin release in the lactating rat. Endocrinology 121:14–20.

Cunningham Jr ET, Sawchenko PE (1988) Anatomical specificity of noradrenergic inputs to the paraventricular and supraoptic nuclei of the rat hypothalamus. J Comp Neurol 274:60–76.

Cunningham Jr ET, Sawchenko PE (1991) Reflex control of magnocellular vasopressin and oxytocin secretion. Trends Neurosci 14:406–411.

Day TA, Renaud LP (1984) Electrophysiological evidence that noradrenergic afferents selectively facilitate the activity of supraoptic vasopressin neurons. Brain Res 303:233–240.

Day TA, Ferguson AV, Renaud LP (1984) Facilitatory influence of noradrenergic afferents on the excitability of rat paraventricular nucleus neurosecretory cells. J Physiol (Lond) 355:237–249.

Day TA, Randle JCR, Renaud LP (1985) Opposing α- and β-adrenergic mechanisms mediate dose-dependent actions of noradrenaline on supraoptic vasopressin neurons *in vivo*. Brain Res 358:171–179.

Douglas AJ, Meeren HK, Johnstone LE, Plaff DW, Russell JA, Brooks PJ (1998) Stimulation of expression of the oxytocin gene in rat supraoptic neurons at parturition. Brain Res 782:167–174.

Dreifuss JJ, Raggenbass M, Charpak S, Dubois-Dauphin M, Tribollet E (1998) A role of central oxytocin in autonomic functions: its action in the motor nucleus of the vagus nerve. Brain Res Bull 20:765–770.

Faull CM, Charlton JA, Butler TJ, Baylis PH (1993) The effect of acute pharmacological manipulation of central serotonin neurotransmission on osmoregulated secretion of arginine vasopressin in the rat. J Endocrinol 139:77–87.

Ginsberg SD, Hof PR, Young WG, Morrison JH (1994) Noradrenergic innervation of vasopressin- and oxytocin-containing neurons in the hypothalamic paraventricular nucleus of the macaque monkey: quantitative analysis using double-label immunohistochemistry and confocal laser microscopy. J Comp Neurol 341:476–491.

Giuliano F, Rampin O (2000) Central neural regulation of penile erection. Neurosci Biobehav Rev 24:517–533.

Grosvenor CE, Mena F (1982) Regulating mechanisms for oxytocin and prolactin secretion during lactation. In: Neuroendocrine perspectives, Vol 1 (Müller EE, MacLeod RM, eds). New York: Elsevier.

Hallbeck M, Blomqvist A (1999) Spinal cord-projecting vasopressinergic neurons in the rat paraventricular hypothalamus. J Comp Neurol 411:201–211.

Huang W, Sjöquist M, Skott P, Stricker EM, Sved AF (2001) Oxytocin antagonist disrupts hypotension-evoked renin secretion and other responses in conscious rats. Am J Physiol Regul Integr Comp Physiol 280:R760–R765.

Iovino M, Steardo L (1985) Effect of substances influencing brain serotonergic transmission on plasma vasopressin levels in the rat. Eur J Pharmacol 113:99–103.

Itoi K, Helmreich DL, Lopez-Figueroa MO, Watson SJ (1999) Differential regulation of corticotropin-releasing hormone and vasopressin gene transcription in the hypothalamus by norepinephrine. J Neurosci 19:5464–5472.

Javed A, Kambradt MC, Van de Kar LD, Gray TS (1999) D-Fenfluramine induces serotonin-mediated Fos expression in corticotropin-releasing factor and oxytocin neurons of the hypothalamus, and serotonin-independent Fos expression in enkephalin and neurotensin of the amygdala. Neuroscience 90:851–858.

Kawata M, McCabe JT, Pfaff DW (1988) *In situ* hybridization histochemistry with oxytocin synthetic oligonucleotide: strategy for making the probe and its application. Brain Res Bull 20:693–697.

Kim YI, Dudley CA, Moss RL (1989) Re-evaluation of the effects of norepinephrine on the single-unit activity of paraventricular neurosecretory neurons. Neurosci Lett 97:103–110.

Larsen PJ, Hay-Schmidt A, Vrang N, Mikkelsen JD (1996) Origin of projections from the midbrain raphe nuclei to the hypothalamic paraventricular nucleus in the rat: a combined retrograde and anterograde tracing study. Neuroscience 70:963–988.

Leibovitz SF, Eidelman D, Suh JS, Diaz S, Sladek CD (1990) Mapping study of noradrenergic stimulation of vasopressin release. Exp Neurol 110:298–305.

Malpas SC, Coote JH (1994) Role of vasopressin in sympathetic response to paraventricular nucleus stimulation in anesthetized rats. Am J Physiol 266:R228–R236.

McLaughlin LL, Wei YF, Stockmann PT, Leahy KM, Needleman P, Grassi J, Pradelles P (1987) Development, validation, and application of an enzyme immunoassay (EIA) of atriopeptin. Biochem Biophys Res Commun 144:469–476.

Meister B, Cortes R, Villar MJ, Schalling M, Hökfelt T (1990) Peptides and transmitter enzymes in hypothalamic magnocellular neurons after administration of hyperosmotic stimuli: comparison between messenger RNA and peptide/protein levels. Cell Tissue Res 260:279–297.

Mikkelsen JD, Jensen JB, Engelbrecht T, Mork A (1999) D-Fenfluramine activates rat oxytocinergic and vasopressinergic neurons through different mechanisms. Brain Res 851:247–251.

Moos F, Richard P (1979) The inhibitory role of β-adrenergic receptors in oxytocin release during suckling. Brain Res 169:595–599.

Plotsky PM (1987) Regulation of hypophysiotrophic factors mediating ACTH secretion. Ann NY Acad Sci 512:205–217.

Porter JP, Brody MJ (1986) Spinal vasopressin mechanisms of cardiovascular regulation. Am J Physiol 251:510–517.

Pradelles P, Grassi J, Maclouf J (1985) Enzyme immunoassays of eicosanoids using acetylcholine esterase as label: an alternative to radio immunoassay. Anal Chem 57:1170–1173.

Randle JC, Day TA, Jhamandas JH, Bourque CW, Renaud LP (1986) Neuropharmacology of supraoptic nucleus neurons: norepinephrine and γ-aminobutyric acid receptors. Fed Proc 45:2312–2317.

Rogers RC, Herman GE (1986) Hypothalamic paraventricular nucleus stimulation-induced gastric acid secretion and bradycardia suppressed by oxytocin antagonist. Peptides 7:695–700.

Sawchenko PE, Swanson LW (1982) The organization of noradrenergic pathways from the brainstem to the paraventricular and supraoptic nuclei in the rat. Brain Res Rev 4:275–325.

Sawchenko PE, Swanson LW, Steinbusch HWM, Verhofstad AAJ (1983) The distribution and cells of origin of the serotonergic inputs to the paraventricular and supraoptic nuclei of the rat. Brain Res 277:355–360.

Saydoff JA, Rittenhouse PA, Van de Kar LD, Brownfield MS (1991) Enhanced serotonergic transmission stimulates oxytocin secretion in conscious male rats. J Pharmacol Exp Ther 257:95–99.

Saydoff JA, Rittenhouse PA, Carnes M, Armstrong J, Van de Kar LD, Brownfield S (1996) Neuroendocrine and cardiovascular effects of serotonin: selective role of brain angiotensin on vasopressin. Am J Physiol 270:E513–E521.

Sherman TG, McKelvy JF, Watson SJ (1983) Vasopressin mRNA regulation in individual hypothalamic nuclei: a Northern and *in situ* hybridization analysis. J Neurosci 6:1685–1694.

Shioda S, Yada T, Muroya S, Takigawa M, Nakai Y (1997) Noradrenaline activates vasopressin neurons via α1-receptor-mediated Ca^{2+} signaling pathway. Neurosci Lett 226:210–212.

Siaud P, Puech R, Assenmacher I, Alonso G (1991) Microinjection of oxytocin into the dorsal vagal complex decreases pancreatic insulin secretion. Brain Res 546:190–194.

Song SL, Crowley WR, Grosvenor CE (1988) Evidence for involvement of an adrenal catecholamine in the β-adrenergic inhibition of oxytocin release in lactating rats. Brain Res 457:303–309.

Stricker EM, Verbalis JG (1986) Interaction of osmotic and volume stimuli in regulation of neurohypophyseal secretion in rats. Am J Physiol Regul Integr Comp Physiol 250:R267–R275.

Tanaka J, Kaba H, Saito H, Seto K (1985) Inputs from the noradrenergic region to hypothalamic paraventricular neurons in the rat. Brain Res 335:368–371.

Tillet Y, Ravault JP, Selve C, Evin G, Castro B, Dubois MP (1986) Conditions for the use of specific antibodies for immunohistochemical visualization of serotonin and melatonin in the pineal gland of sheep (in French). C R Acad Sci III 303:77–82.

Tillet Y, Batailler M, Krieger-Poullet M, Thibault J (1990) Presence of dopamine-immunoreactive cell bodies in the catecholaminergic group A15 of the sheep brain. Histochemistry 93:327–333.

Tracer HL, Loh YP (1993) The effect of salt loading on corticotropin-releasing hormone and arginine vasopressin mRNA levels in the mouse hypothalamus: a quantitative *in situ* hybridization analysis. Neuropeptides 25:161–167.

Trembleau A, Roche D, Calas A (1993) Combination of non-radioactive and radioactive *in situ* hybridization with immunohistochemistry: a new method allowing the simultaneous detection of two mRNAs and one antigen in the same brain tissue section. J Histochem Cytochem 41:489–498.

Tribollet E, Clarke G, Dreifuss JJ, Lincoln DW (1978) The role of central adrenergic receptors in the reflex release of oxytocin. Brain Res 142:69–84.

Van Tol HHM, Voorhuis DTAM, Burbach JPH (1987) Oxytocin gene expression in discrete hypothalamic magnocellular cell groups is stimulated by prolonged salt loading. Endocrinology 120:71–76.

Vicentic A, Li Q, Battaglia G, Van de Kar LD (1998) WAY-100635 inhibits 8-OH-DPAT-stimulated oxytocin, ACTH and corticosterone, but not prolactin secretion. Eur J Pharmacol 346:261–266.

Willoughby JO, Jervois PM, Menadue MF, Blessing WW (1987) Noradrenaline, by activation of α1 adrenoreceptors in the region of the supraoptic nucleus, causes secretion of vasopressin in the anaesthetized rat. Neuroendocrinology 45:219–226.

Yamashita H, Inenaga K, Kannan H (1987) Depolarizing effect of noradrenaline on neurons of the rat supraoptic nucleus *in vitro*. Brain Res 405:348–352.

Zingg HH, Lefebvre DL (1988) Oxytocin and vasopressin gene expression during gestation and lactation. Brain Res 464:1–6.